scientific reports

Check for updates

OPEN

Identification of diagnostic and prognostic genetic alterations in uveal melanoma using RNA sequencing

Rogier J. Nell[1]✉, Mieke Versluis[1], Davy Cats[2], Hailiang Mei[2], Robert M. Verdijk[3,4], Wilma G. M. Kroes[5], Gregorius P. M. Luyten[1], Martine J. Jager[1] & Pieter A. van der Velden[1]

Uveal melanoma is a lethal intraocular tumour, in which the presence of various genetic alterations correlates with the risk of metastatic dissemination and survival. Here, we tested the detectability of all key mutations and chromosomal changes from RNA sequencing data in 80 primary uveal melanomas studied by The Cancer Genome Atlas (TCGA) initiative, and in five prospective cases. Whereas unsupervised gene expression profiling strongly indicated the presence of chromosome 3 alterations, it was not reliable in identifying other alterations. Though, the presence of both chromosome 3 and 8q copy number alterations could be successfully inferred from expressed allelic imbalances of heterozygous common single nucleotide polymorphisms. Most mutations were adequately recognised in the RNA by their nucleotide changes (all genes), alternative splicing around the mutation (*BAP1*) and transcriptome-wide aberrant splicing (*SF3B1*). Notably, in the TCGA cohort we detected previously unreported mutations in *BAP1* (n = 3) and *EIF1AX* (n = 5), that were missed by the original DNA sequencing. In our prospective cohort, all genetic alterations were successfully identified by combining the described approaches. In conclusion, a transcriptional analysis presents insights into the expressed tumour genotype and its phenotypic consequences and may augment or even substitute DNA-based approaches, with potential applicability in research and clinical practice.

Keywords Uveal melanoma, Genetic profiling, RNA sequencing

Uveal melanoma is a lethal intraocular tumour characterised by a high metastatic rate and limited treatment options once disseminated[1]. In contrast to most other malignancies, it presents as a relatively simple genetic disease with a low mutational burden and limited number of structural variants[2,3]. Practically all tumours harbour a mutually-exclusive mutation in *GNAQ*, *GNA11*, *CYSLTR2* or *PLCB4*, which activates the $G\alpha_q$ signalling pathway[4–7]. Most uveal melanomas also carry a so-called BSE (*BAP1*, *SF3B1* or *EIF1AX)* mutation[2,8–10]. Copy number losses of chromosome 3 and increases of chromosome 8q are the most prevalent structural alterations, and occur in specific combinations together with the BSE mutations. These various molecular subtypes have been associated with distinct gene expression profiles (GEP) and are differentially correlated to the risk of early metastatic dissemination and consequent patient survival (Table 1).

The prognostic value of genetic alterations in uveal melanoma has been recognised for more than two decades. Traditionally, copy number alterations were studied using cytogenetic techniques, such as karyotyping, fluorescence in situ hybridisation, multiplex ligation-dependent probe amplification and array genotyping[11–15]. Technical advancements enabled genome-wide analyses by next-generation sequencing and led to the discovery of recurrent mutations[2,8–10]. Nowadays, (targeted) sequencing can be used to detect all relevant alterations—both copy number alterations and mutations—in one single analysis [16,17].

In addition to these DNA-based approaches, several studies have identified clinically-relevant transcriptional subtypes of uveal melanoma. Most commonly, tumours are divided into class I or II based on their bulk GEP. This classification can be established using dimensionality reduction and sample clustering techniques of total RNA expression data, or by evaluating expression variation in a selection of genes[18–21]. Intriguingly, this

[1]Department of Ophthalmology, Leiden University Medical Center, PO Box 9600, 2300 RC Leiden, The Netherlands. [2]Department of Biomedical Data Sciences, Leiden University Medical Center, Leiden, The Netherlands. [3]Department of Pathology, Leiden University Medical Center, Leiden, The Netherlands. [4]Department of Pathology, Erasmus University Medical Center, Rotterdam, The Netherlands. [5]Department of Clinical Genetics, Leiden University Medical Center, Leiden, The Netherlands. ✉email: r.j.nell@lumc.nl

GEP	Mutations	Copy number alterations	Risk to (early) metastasis
Class I	$G\alpha_q$ + *EIF1AX*		Low
	$G\alpha_q$ + *SF3B1*	+ 8q	Intermediate
Class II	$G\alpha_q$ + *BAP1*	− 3, + 8q	High

Table 1. Summary of three most typical combinations of GEP classification, mutations, chromosomal copy number alterations and their correlation to the risk of (early) metastatic dissemination[1].

transcriptional classification is known to correlate with the presence of genetic alterations affecting chromosome 3 (i.e. with monosomy 3 and *BAP1* mutations restricted to GEP class II, Table 1). Given that part of the bulk GEP may be derived from admixed non-malignant cells, such as tumour-infiltrating immune cells, RNA data can also provide insights into the tumour microenvironment of uveal melanomas[22,23].

More recently, the presence and consequences of genetic alterations at the transcriptional level have gained interest in the context of uveal melanoma. Mutations in *SF3B1*, a gene encoding for a core component of the cell's splicing machinery, were found to lead to a recurrent profile of aberrant splice junction usage[2,24]. As another example, in three large-scale genomic studies, a variety of complex *BAP1* alterations were only identified after using RNA sequencing data in addition to DNA-derived data[21,25,26]. Finally, *CYSLTR2*-mutant uveal melanomas recurrently showed silencing of the wild-type allele and preferential expression of the p.L129Q mutation[27]. These examples emphasise the value of investigating RNA in addition to DNA to identify the presence and consequences of certain genetic alterations.

In this study, we apply various bioinformatic approaches to detect all key genetic alterations in uveal melanoma by only using tumour-derived RNA sequencing data. Cohort-wide GEP is used to identify class I and II tumours. In individual samples, copy number alterations are analysed by measuring expressed allelic imbalances of heterozygous common single nucleotide polymorphisms (SNPs). Mutations are identified by screening of hotspot regions and by evaluating their transcriptional effects. Our findings are validated by comparing them to DNA-derived data in a training cohort of 80 primary uveal melanomas originally studied by The Cancer Genome Atlas (TCGA) initiative, and in five prospectively analysed cases from our institution.

Results

Estimation of genetic alterations via cohort-wide gene expression profiling

The RNA-derived classification of primary uveal melanomas into GEP class I or II is originally based on unsupervised clustering of transcriptome-wide expression data into two groups[19,20]. Concordantly, a dimensionality reduction analysis (uniform manifold approximation and projection, UMAP) successfully divided the TCGA tumours (n = 80) into two main clusters based on their total transcriptional diversity (Fig. 1A). To investigate expression patterns underlying this subdivision, we inferred a signature of 200 genes characterising the two clusters. The largest proportion (82/200, 41%) of these genes were located on chromosome 3 (Fig. 1B and Supplementary Table 1), with systematically lower levels of expression in one cluster of tumours (n = 40, marked as GEP class II) relative to the other (n = 40, marked as GEP class I). This classification almost completely overlapped with the true DNA-determined copy number status of chromosome 3: 40/40 GEP class II tumours demonstrated loss of this chromosome (i.e. monosomy, or isodisomy in polyploid melanomas), compared to 3/40 GEP class I tumours (Fig. 1C and Supplementary Table 2). The three discordant cases were the only tumours showing arm-level variation of chromosome 3 loss (n = 2) or an unusual trisomy 3 in the context of polyploidy (n = 1, Supplementary Fig. 1A and B). In line with the frequent co-occurrence of chromosome 3 copy number losses and *BAP1* alterations, mutations in *BAP1* were present in 40/40 GEP class II and 0/40 GEP class I tumours (Fig. 1C and Supplementary Table 2).

In contrast, cohort-wide GEP clustering did not specifically overlap with the presence of chromosome 8q copy number changes or other mutations, even not after specifying the analysis to class I or II tumours only (Fig. 1C and Supplementary Fig. 2). These observations suggest that alternative approaches are needed to infer all (clinically-)relevant genetic alterations from RNA data.

Identification of copy number alterations via RNA-expressed allelic imbalances

To detect chromosomal copy number alterations in individual tumours, we proceeded by measuring regional allelic imbalances in the RNA sequencing data. For this goal, highly expressed heterozygous common SNPs were identified and their so-called B-allele fractions (BAFs) were visualised according to their chromosomal positions. These values refer to the measured expression of one allele compared to the total expression of both alleles. Under copy number neutral conditions, two alleles—and thus both SNP variants—are equally abundant, resulting in BAFs of ~ 50% (Fig. 2A). In contrast, a chromosomal loss, such as monosomy 3, typically leads to BAFs close to ~ 0% and ~ 100%, as it is caused by an (almost) complete loss of one of the two alleles ('loss of heterozygosity', Fig. 2B). Using this approach, we were able to correctly identify disomic tumours (n = 40, with preserved balanced expression) and tumours with (partial) loss of chromosome 3 (n = 39, showing imbalanced expression) from the RNA sequencing data in 79/80 (99%) cases of the TCGA cohort (Fig. 2C and Supplementary Table 2). The only conflicting case was the one presenting with an unusual trisomy 3 in the context of polyploidy, which was also characterised by an allelic imbalance (Supplementary Fig. 1B).

This latter case illustrates that, similar to chromosomal losses, copy number increases typically also lead to allelic imbalances. A gain, such as of chromosome 8q (or chromosome 3 in the discordant case described above), is usually the result of an extra copy of one allele, leading to BAFs around ~ 67% and ~ 33% (Fig. 2A). Larger

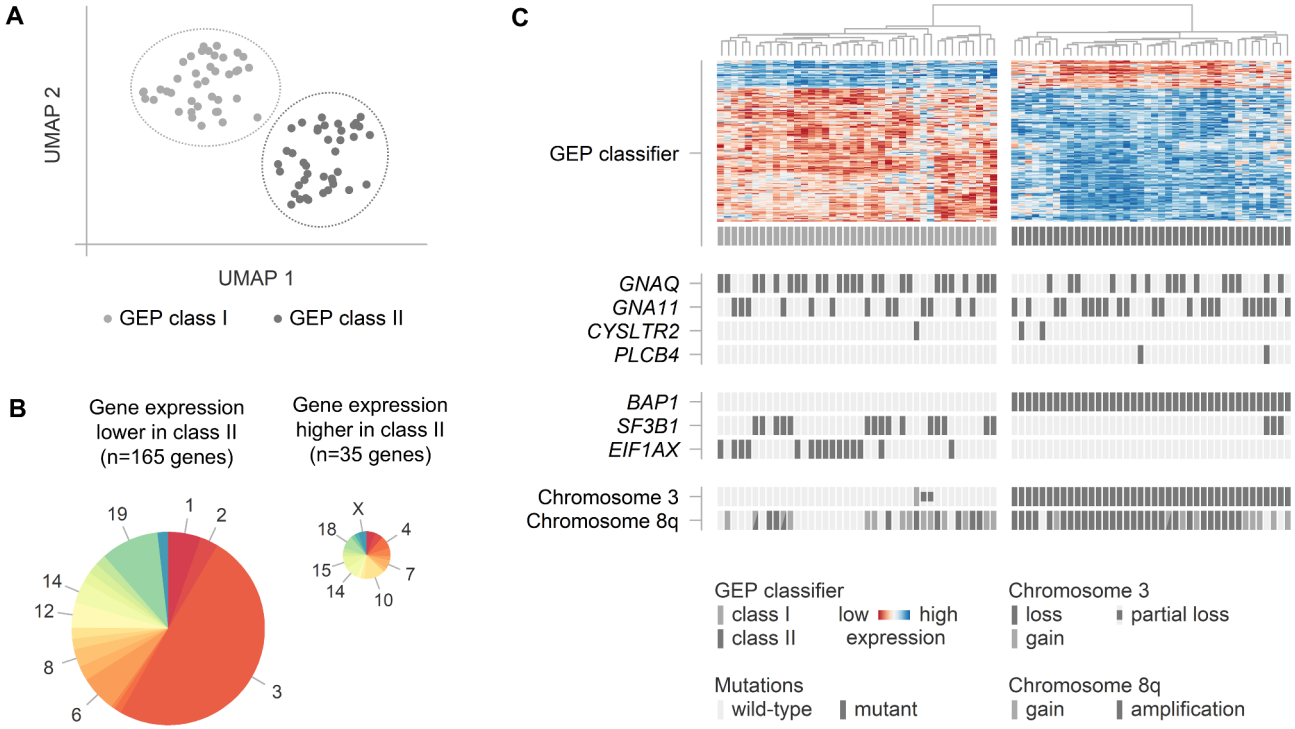

Fig. 1. Cohort-wide GEP to estimate the presence of genetic alterations in our training cohort of uveal melanomas studied by TCGA (n = 80). (**A**) Two-dimensional UMAP analysis to identify two clusters of tumours: GEP class I and II. (**B**) Chromosomal location of signature genes characterising the two clusters. (**C**) Relative gene expression levels of signature genes characterising the two clusters in relation to the genetic alterations present per individual tumour.

amplifications mostly originate from several copies of one allele (with BAFs > 67% and < 33%, Fig. 2B). On the other hand, amplifications derived from extra copies of both alleles or subclonal alterations result in BAFs closer to 50% and may be more difficult to recognise (Supplementary Fig. 1C). In the TCGA cohort, chromosome 8q allelic imbalances were detected in the RNA sequencing data of 53 tumours, which all had a DNA-confirmed gain or amplification of chromosome 8q. The remaining 27 cases lacked measurable BAF deviations, and could be explained by a disomy 8q (n = 21) or a copy number increase of both alleles (n = 6). In aggregate, the presence or absence of any 8q alteration was correctly identified from RNA sequencing data in 74/80 (93%) of these uveal melanomas (Fig. 2C and Supplementary Table 2).

Of note, depending on the number of informative SNPs and their clonality in individual tumours, regional allelic imbalances involving other chromosomes were also successfully identified by this approach (Fig. 2A, B).

RNA-based identification of $G\alpha_q$ and BSE mutations

Next, we aimed to identify the mutational status of individual uveal melanomas at the transcriptional level (Fig. 3A and Supplementary Table 2). $G\alpha_q$ signalling mutations are known to occur at a selected number of hotspots (p.G48, p.R183 and p.Q209 for *GNAQ* and *GNA11*, p.L129 for *CYSLTR2* and p.D630 for *PLCB4*[4–7]), allowing for a targeted analysis of RNA sequencing data (Fig. 3B). Though, due to a lack of sequencing reads covering the mutant positions, DNA-confirmed *GNAQ* mutations could not be adequately detected in the RNA data of four cases (Supplementary Fig. 3A). Still, the $G\alpha_q$ mutations were correctly identified in the remaining 74/78 (95%) mutant uveal melanomas (Fig. 3A and Supplementary Table 2).

BAP1 alterations are typically inactivating mutations (or deletions) that can be present throughout the complete *BAP1* gene. This challenges the identification of all alterations using conventional sequencing[25,26]. In the TCGA cohort of uveal melanomas, it was earlier shown that various complex (intronic) *BAP1* alterations can be identified by the use of RNA sequencing[21,25]. However, exonic missense and nonsense mutations are also detectable at the transcriptional level: directly via their nucleotide changes, or indirectly via observed alternative splicing events such as (partial) intron retention or exon skipping (Fig. 3C). With these RNA-based evaluations, we identified three mutations that had remained unrecognised in previous studies (p.W196X in VD-A8KM, a deletion involving the start of exon 1 in V4-A9ES, and a frameshift deletion involving exon 8 in WC-A883, Fig. 3C and Supplementary Fig. 3B and C). In line with the expected tumour genotypes, these *BAP1* mutations were found in cases with monosomy 3 (Supplementary Table 2). In two other tumours, the *BAP1* mutations were only identified at the DNA level due to a low number of mutant RNA sequencing reads (Supplementary Fig. 3A). Taken together, 38/40 (95%) *BAP1* mutations could be detected via RNA sequencing (Fig. 3A and Supplementary Table 2).

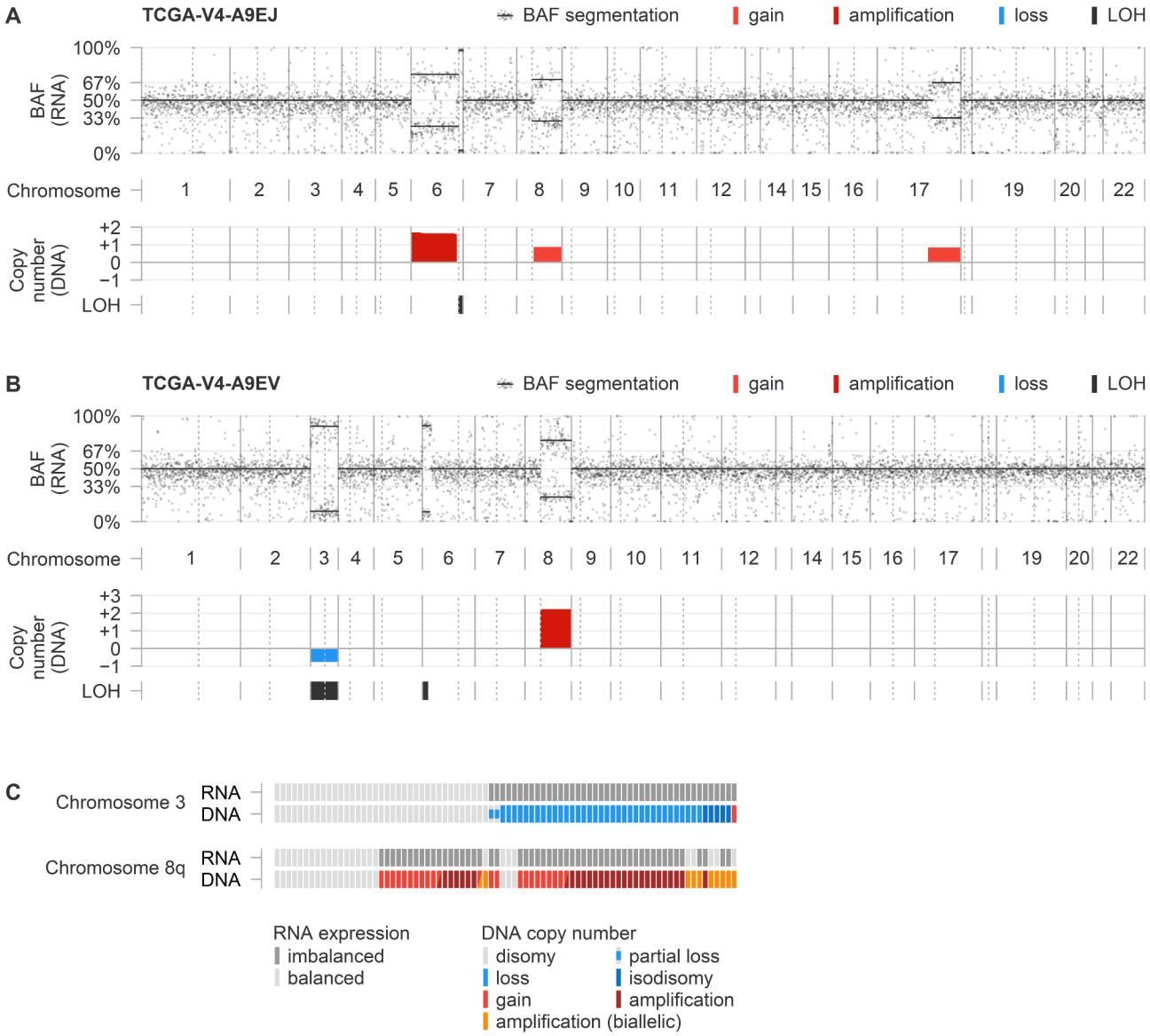

Fig. 2. RNA-inferred allelic imbalances in relation to DNA-confirmed copy number alterations. The figures for all TCGA tumours can be found in Supplementary Data 1. (**A**) Example of a tumour showing balanced expression of chromosome 3, but imbalanced expression of chromosome 8q, in line with a disomy 3 and copy number alteration of chromosome 8q. Additionally, alterations affecting chromosome 6p, 6q and 17q (partial) are correctly identified. (**B**) Example of a tumour showing imbalanced expression of both chromosome 3 and 8q, in line with copy number alterations of the two chromosomes. Additionally, an alteration affecting chromosome 6p (partial) is correctly identified. (**C**) Overview of our RNA-derived observations in comparison with the DNA-determined copy number values in the 80 TCGA tumours. Balanced expression correctly identified all tumours with disomy 3 (n = 40/40), and imbalanced expression nearly always meant the tumour had lost (part) of chromosome 3 (n = 39/40). Concerning chromosome 8q, most tumours with balanced expression had a disomy 8q (n = 21/27), and all tumours with imbalanced expression had a gain or amplification of this chromosome (n = 53/53). In aggregate, the presence or absence of a copy number loss of chromosome 3 or increase of 8q was correctly identified from RNA sequencing data in 79/80 (99%) and 74/80 (93%) of the uveal melanomas.

SF3B1 mutations in uveal melanomas are predominantly found in exon 14, with most of them affecting positions p.R625 or p.K666[2,9,10,24]. We successfully identified 14/15 (93%) DNA-confirmed mutations by nucleotide variation in the RNA sequencing data of the TCGA cohort (Fig. 3A, D and Supplementary Table 2), with again a limited number of reads at the mutant position in the discordant tumour (Supplementary Fig. 3A). However, by evaluating a recurrent profile of aberrant splice junction usage caused by *SF3B1* mutations[2,24], alternative splicing was found in all 15/15 (100%) mutant tumours (and none of the wild-type samples, Fig. 3E).

EIF1AX mutations mainly affect the N-terminal region of the gene, spanning the first two exons with a total of fifteen amino acids [10]. In the TCGA dataset, we detected the presence of a DNA-confirmed *EIF1AX* mutation in the RNA of 9/10 tumours, with—similar to the missed *GNAQ* mutation in the same tumour—a lack of sequencing reads explaining the discordant sample (Supplementary Fig. 3A). However, we also observed that there was practically no coverage of exon 1 in the exome-captured DNA sequencing data, and none of the TCGA tumours was known to have an exon 1 mutation [21]. By analysing the (uncaptured) RNA sequencing data (Fig. 3F), we identified expressed exon 1 mutations in five TCGA cases (p.P2H in VD-AA8M, p.P2L in YZ-A983, p.P2R in V4-A9EH, p.K3N in WC-A87T, and p.N4S in VD-AA8Q). All these tumours further presented with disomy of chromosomes 3 and 8q and lacked mutations in *SF3B1* or *BAP1*, in line with the typical genotype of *EIF1AX*-mutant tumours. For two cases, low-pass whole genome sequencing was available and confirmed both mutations (Supplementary Fig. 3D). Taken together, 14/15 (93%) *EIF1AX* mutations were successfully identified at the RNA level, including five previously missed with DNA-based exome sequencing (Fig. 3A and Supplementary Table 2).

Prospective validation of RNA-based detectability of genetic alterations

Finally, we aimed to prospectively validate all beforementioned techniques in an independent cohort. For this goal, we performed RNA sequencing of five primary uveal melanoma specimens obtained after enucleation in our hospital (Fig. 4 and Supplementary Table 3). The presence of chromosome 3 and 8q copy number alterations, and $G\alpha_q$ and BSE mutations was confirmed at the DNA level using digital PCR and targeted sequencing, and—for BAP1—at the protein level using immunohistochemistry.

Although the number of tumours in our cohort was too low to reliably determine the GEP classification based on unsupervised clustering (Fig. 4A), three tumours were found to be GEP class I and two tumours were GEP class II upon evaluation of our TCGA-based 200-gene expression signature. This classification matched with the loss of heterozygosity of chromosome 3 in the RNA sequencing data (exemplified in Fig. 4B). Additionally, three tumours showed allelic imbalances of chromosome 8q. The presence of all these presumed copy number alterations could be successfully validated at the DNA level.

Regarding the $G\alpha_q$ mutations, all five tumours expressed one hotspot mutation in *GNAQ* (n = 4) or *GNA11* (n = 1, Fig. 4B). Next, the RNA data demonstrated the presence of BSE mutations in *BAP1* (n = 2), *SF3B1* (n = 2) and *EIF1AX* (n = 1). The *BAP1* mutations caused RNA-detectable nucleotide variation as well as altered splicing around the mutated sites, showing high similarities to TCGA tumours with comparable mutations (Fig. 4C). The tumours with the *SF3B1* p.R625 hotspot mutations were the ones demonstrating *SF3B1*-associated aberrant splicing (Fig. 4D). One tumour carried an *EIF1AX* mutation affecting exon 2. All mutations could be verified at the DNA level. Additionally, the presence and pathogenicity of the *BAP1* alterations was supported by a negative (n = 2) or positive (n = 3) BAP1 nuclear staining (Supplementary Table 3).

Taken together, all measured copy number alterations and mutations were correctly identified in the RNA sequencing data of the five uveal melanomas.

Discussion

Uveal melanoma is characterised by a number of prognostically-relevant combinations of genetic alterations, that are mostly measured at the DNA level. In this study, we tested whether these alterations could also be detected at the transcriptional level using RNA sequencing data. This identification of mutations and copy number alterations was validated in comparison to DNA-based techniques in both a retrospective cohort of 80 TCGA tumours and five prospectively analysed uveal melanomas from our own cohort.

First of all, we explored the indirect detectability of genetic alterations via unsupervised GEP clustering, a commonly-used procedure in the context of classifying uveal melanoma. Our analysis revealed—in line with earlier studies—two main groups of tumours which overlapped with the absence or presence of chromosome 3 alterations (complete chromosomal loss and *BAP1* mutation, Figs. 1 and 4A). Indeed, a large number of genes on chromosome 3 was expressed systematically lower in bulk RNA upon loss of this chromosome. However, GEP clustering was influenced by the extent of chromosome 3 loss (i.e. partial losses were not identified) and could not be used to specify the exact *BAP1* mutation. It also did not identify chromosome 8q copy number alterations or any of the other recurrent and relevant mutations, such as those in *SF3B1* and *EIF1AX*. As a further drawback, the GEP approach intrinsically relies on differences observed within a cohort, between multiple tumours. This makes this analysis less applicable to separate tumours, as it always requires a comparison to other samples (or 'normal' values) to identify any variation. For this reason, we further focussed on alternative approaches applicable to data of individual uveal melanomas.

To better identify chromosomal alterations, we measured regionally-abundant allelic imbalances of heterozygous common SNPs detectable in RNA data (Fig. 2). This approach has several similarities to a DNA-based methodology we presented and discussed recently[28]. Based on (partial) copy number losses of chromosome 3, expressed loss of heterozygosity could be observed at the transcriptional level and turned out to be an excellent marker for this genetic event. The other way round, chromosome 8q copy number increases, predominantly mono-allelic gains or amplifications, were also readily detected by allelic imbalances present in RNA. Advantageously, by selecting highly expressed SNPs known to be frequently heterozygous in the population, the analysis could be performed directly from RNA data and no patient-matched genotype information was required. Because of the existence of (cellular) heterogeneity, even a complete loss of heterozygosity in malignant cells may be detected due the presence of admixed heterozygous non-malignant cells. As an example, we successfully identified all cases with loss of chromosome 3, which is typically a clonally-abundant copy number alteration, but found in tumours with the lowest purity of all uveal melanomas (mainly due to infiltrating non-malignant immune cells)[22,23,29].

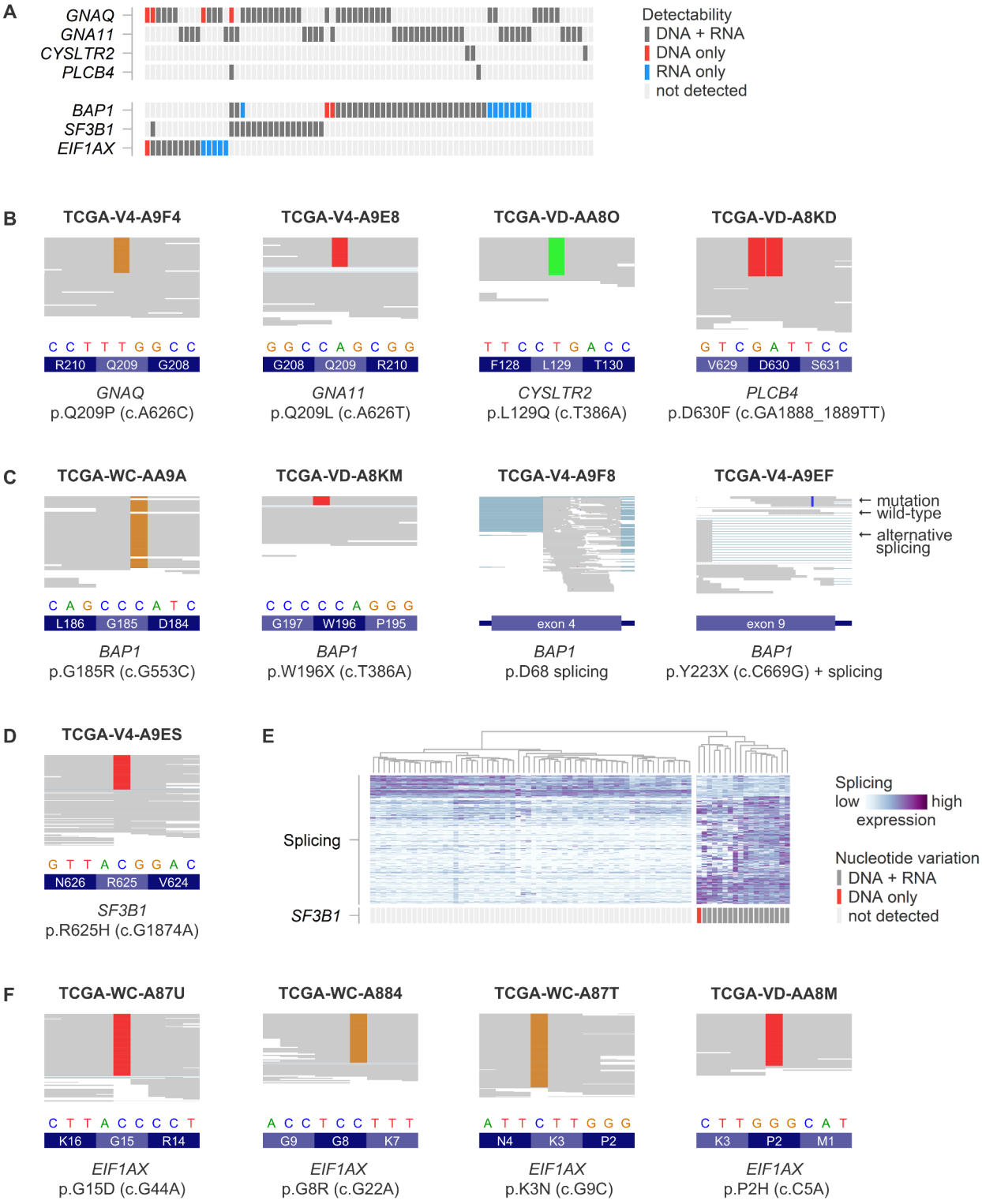

To detect BSE mutations at the RNA level, all mutational hotspot regions were screened and possible transcriptional consequences of various alterations (i.e. alternative splicing) were evaluated (Fig. 3). Although a small number of mutations were missed due to insufficient sequencing coverage, the large majority was successfully detected in the RNA data. Interestingly, this included three additional *BAP1* mutations and five *EIF1AX* mutations in the TCGA cohort that were previously unrecognised as part of the respective genes were not or not sufficiently covered by the exome-captured DNA sequencing. Clinically, these alterations are prognostically relevant and not to be missed in any routine mutational screening of a uveal melanoma, substantiating complete coverage in any (targeted) sequencing panel. It is also essential that these alterations are known and being taken into account when analysing mutation data from these TCGA tumours in a research setting.

◀**Fig. 3**. Detectability of mutations via RNA sequencing data in our training cohort of uveal melanomas studied by TCGA (n = 80). All details are described in Supplementary Table 2. (**A**) Summary of detected mutations in comparison to findings in exome-captured DNA sequencing. At the RNA level, $G\alpha_q$ mutations were correctly identified in 74/78 (95%), *BAP1* mutations in 38/40 (95%), *SF3B1* mutations in 15/15 (100%) and *EIF1AX* mutations in 14/15 (93%) mutant uveal melanomas. Note that various mutations were missed by the initial DNA-based analyses and detected by RNA sequencing only. (**B**) Examples of detected $G\alpha_q$ signalling mutations in RNA sequencing data. (**C**) Examples of detected *BAP1* mutations in RNA sequencing data: although some were identified directly via nucleotide variation, others showed alternative splicing around the mutant position. (**D**) Example of detected *SF3B1* mutation in RNA sequencing data. (**E**) *SF3B1*-mutant tumours are known to result in a recurrent profile of aberrant splice junction usage [2,24]. This signature of alternative splicing was effectively used to identify *SF3B1*-mutant tumours in the TCGA cohort. (**F**) Examples of detected *EIF1AX* mutations in RNA sequencing data.

Though most mutations were directly recognised from nucleotide changes visible in the RNA sequencing reads, a number of *BAP1* mutations were identified via unusual splicing events within this gene (Figs. 3C and 4C). In some tumours, the splice site disruption may be directly caused by the mutation being located near a regular exon–intron boundary, or the mutation introducing a novel splice site. Other tumours showed evidence of 'nonsense-associated alternative splicing': (partial) exon skipping or intron retention, apparently in response to the premature translation-termination codons introduced by nonsense or frameshift mutations. In contrast to nonsense-mediated decay, in-frame alternative splicing bypassing the original mutation might encode for a protein with saved functionalities, even though the mutation is predicted to be truncating and highly pathogenic[30,31]. Our observations—possibly explainable by these phenomena, but yet to be followed up at a functional level—further contribute to the notorious complexity of *BAP1* alterations and their biological consequences[16,17,32–34].

Critically, our current study is limited by its relatively low number of prospectively validated cases from independent cohorts. Still, the validation with DNA-based results in a total of 85 tumours (i.e. the TCGA and our own cohort combined) strongly suggests that most relevant alterations in uveal melanoma can be detected at the transcriptional level, especially when various bioinformatic approaches are combined. This indicates that RNA sequencing data, newly or retrospectively collected for gene expression analysis, may be mined for genetic alterations without the need to perform additional DNA-based measurements. Moreover, it may allow researchers to study genotype–phenotype relations in the same tumour specimen in more detail. This is particularly interesting in the context of measuring genetic heterogeneity next to transcriptional heterogeneity, for example using multiregional or single-cell RNA sequencing. Thirdly, the detectability of genetic alterations in the RNA of uveal melanomas may provide the rationale to study (cell-free) RNA from liquid biopsies, which already showed potential in other types of cancer[35–38].

In a follow-up study, our evaluations may be extended to other genetic alterations in uveal melanoma. Besides chromosome 3 and 8q, (partial) copy number alterations affecting chromosome 1, 6 and 16 are recurrently present and—although not extensively validated—were already correctly observed as allelic imbalances in some of our tumours (Fig. 2 and Supplementary Fig. 1). Additionally, mutations in splicing factor *SRSF2*, which seem to form a rare alternative to *SF3B1* mutations[21,39], might be recognised in the RNA sequencing reads or by its own signature of alternative splicing. Moreover, it would be therapeutically relevant to evaluate alterations involving *MBD4*. Biallelic inactivation of this gene (via a mutation and copy number loss of its locus on chromosome 3) has been identified as a rare cause of CpG to TpG hypermutation in uveal melanoma, conferring unique sensitivity to immunotherapy[40,41]. Next to identifying mutations at the RNA level, additional evidence for MBD4 inactivation can be found in an unusually high total mutational burden, which might also be inferred from RNA sequencing data[42]. Finally, our methodologies might be valuable beyond the field of uveal melanoma, and it would be interesting to evaluate these in other types of cancer.

In conclusion, we developed and applied a variety of bioinformatic approaches showing that transcriptional data—in addition to providing gene expression levels and profiles—forms a rich source of (clinically-)relevant genetic information in uveal melanoma. Via RNA, valuable insights could be obtained into the expressed genotype and its phenotypic consequences, but this also demonstrated the vulnerabilities of an (insufficiently) targeted DNA measurement. As illustrated by the identification of previously unreported mutations in the thoroughly studied TCGA cohort, and the successful prospective analysis of tumours of our own cohort, the analysis of transcriptional data may augment or even substitute current DNA-based approaches, and has potential applicability in both oncological research and clinical practice.

Methods

Collection and analysis of retrospective cohort

RNA sequencing files from the 80 primary uveal melanomas studied by the TCGA[13] were downloaded from the NCI Genomic Data Commons data portal (GDC; https://portal.gdc.cancer.gov). After reconversion to FASTQ files using samtools (version 1.1), the reads were aligned using STAR (version 2.5.3a) to human reference genome GRCh38. Gene counts were generated using htseq-count (version 0.6.0) and annotated with Ensembl (version 87). DESeq2 (version 1.30.0) was used for variance stabilising transformation of the count data, which formed the input for the UMAP analysis. An expression signature of 200 genes characterising the two visually separated clusters was identified using ClaNC, and was used to classify tumours as 'class I' or 'class II' based on the relative expression of chromosome 3 genes (i.e. high or low, respectively).

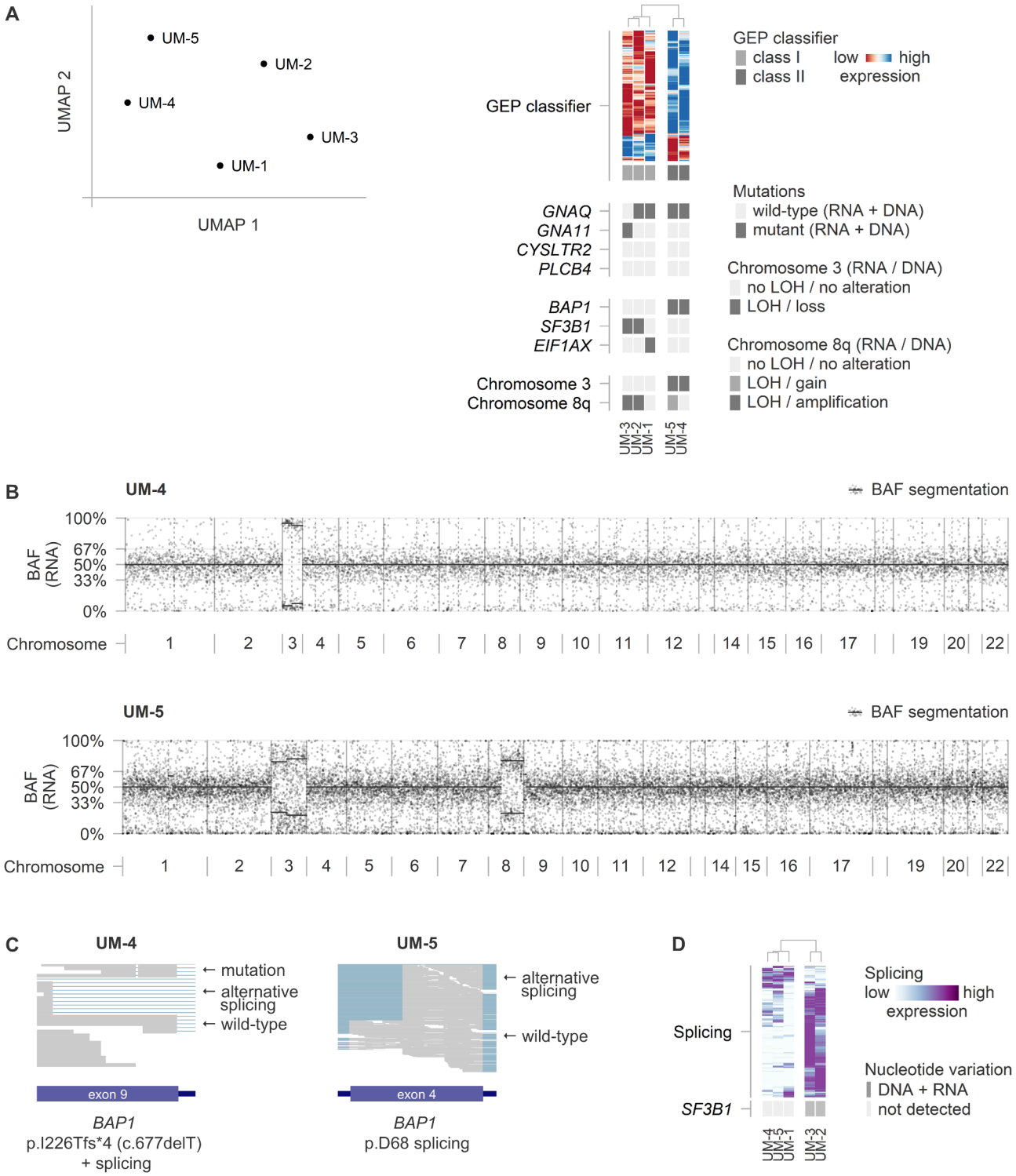

Fig. 4. Analysis of our prospective cohort of uveal melanomas (n = 5). (**A**) Two-dimensional UMAP analysis of cohort-wide GEP and application of TCGA-derived GEP-classifier in relation to the RNA- and DNA-based detectability of genetic alterations. (**B**) Representative examples of RNA-inferred allelic (im)balances to identify chromosomal alterations. In UM-4 and UM-5, imbalanced expression of genes of chromosome 3 correctly indicates the presence of a copy number alteration affecting this chromosome. In contrast, in UM-4, no imbalance is observed on chromosome 8q, in line with a disomy 8q, but an alteration and consequent imbalance is present in UM-5. The figures for all tumours from our cohort can be found in Supplementary Data 2. (**C**) *BAP1* alterations (mutations and mutation-associated alternative splicing) as observed in the RNA sequencing data. (**D**) Analysis of the previously described signature of alternative splicing to identify *SF3B1*-mutant tumours.

The aligned RNA sequencing files were analysed for variants using VarScan (version 2.3), which were annotated using snpEff/snpSift (version 5.1) according to dbSNP (version 151).

To visualise allelic (im)balances without having patient-matched germline genotype information available, only heterozygously and highly expressed common SNPs (flagged as 'common', total number of reads > 40, number of reference reads > 2, number of alternate reads > 2) were included in the downstream analysis. For all SNPs, the fractions alternate reads of total reads were visualised according to their chromosomal positions. Segmentation was performed manually. RNA-derived allelic (im)balances were compared to DNA-measured copy number information determined from Affymetrix SNP 6.0 arrays, available from the Pan-Cancer Atlas initiative[43] (https://gdc.cancer.gov/about-data/publications/pancanatlas).

All aligned RNA sequencing files were further screened for (hotspot) mutations in *GNAQ* (p.Q209, p.R183 and p.G48), *GNA11* (p.Q209, p.R183), *CYSLTR2* (p.L129), *PLCB4* (p.D630), *EIF1AX* (entire gene), *SF3B1* (exon 14) and *BAP1* (entire gene) using freebayes (version 1.3.6), and via manual inspection using the Integrative Genomics Viewer (version 2.8.10). At least two concordant alternate reads at any of the driver gene hotspots were required to call a mutation. The presence of mutations was compared to those detectable in aligned DNA sequencing files generated by exome-captured sequencing (n = 80) or low-pass whole-genome sequencing (n = 51) downloaded from the GDC data portal.

The bioinformatic analyses were carried out using R (version 4.0.3) and RStudio (version 1.4.1103). All custom scripts are available via https://github.com/rjnell/um-rna.

Collection, isolation and analysis of prospective cohort

Five snap-frozen primary uveal melanoma specimens were collected from the biobank of the Department of Ophthalmology, Leiden University Medical Center (LUMC). These samples were originally obtained from patients treated by an enucleation in the LUMC. This study was approved by the LUMC Biobank Committee and Medisch Ethische Toetsingscommissie under numbers B14.003/SH/sh and B20.026/KB/kb, and due to its retrospective nature, the need of obtaining informed consent was waived. The study was performed in accordance with local and national regulations and the principles described in the Declaration of Helsinki.

RNA from all specimens (25 × 20 µm sections) was isolated using the QIAamp RNeasy Mini Kit (Qiagen, Hilden, Germany), following the manufacturer's instructions. 100 ng of RNA per sample was sequenced by GenomeScan (Leiden, the Netherlands). Sample preparation was performed using the NEBNext Ultra Directional RNA Library Prep Kit for Illumina (New England Biolabs, Ipswich, USA) according to the NEB #E7240S/L protocol. In short, mRNA was isolated from total RNA using oligo-dT magnetic beads. After fragmentation of the mRNA, cDNA synthesis was performed and used for ligation with the sequencing adapters and PCR amplification. Quality and yield were measured with the Fragment Analyzer (Agilent, Santa Clara, USA). Next, clustering and DNA sequencing was performed using the cBot and HiSeq 4000 (Illumina, San Diego, USA) according to the manufacturer's protocols. HiSeq control and image analysis, base calling and quality check were carried out using HCS (version 3.4.0), the Illumina data analysis pipeline RTA (version 2.7.7) and bcl2fastq (version 2.17). The raw sequencing files underwent the same alignment and analysis pipeline as the TCGA data files to perform GEP clustering and infer copy number alterations and mutations.

DNA from uveal melanomas (25 × 20 µm sections) was isolated with the QIAmp DNA Mini Kit (Qiagen) according to the manufacturer's instructions. Digital PCR was performed to measure the copy number values of chromosome 3 and 8q and to confirm mutations in *GNAQ*, *GNA11*, *EIF1AX* and *SF3B1*. These experiments were carried out using the QX200 Droplet Digital PCR System (Bio-Rad Laboratories, Hercules, USA) following established protocols[22,27,28,44,45], and two new assays listed in Supplementary Table 4. The presence and pathogenicity of *BAP1* alterations was confirmed by targeted Sanger or next-generation sequencing and an immunohistochemical staining, both performed as routine diagnostic analyses in two ISO accredited laboratories (Departments of Clinical Genetics and Pathology, LUMC)[16,46].

Data availability

All processed results generated in this study are available within the manuscript and its Supplementary Information. The raw data are not openly available due to reasons of sensitivity. Controlled access sequencing data from the 80 primary uveal melanomas studied by the TCGA were downloaded from the NCI Genomic Data Commons data portal (https://portal.gdc.cancer.gov, dbGaP Study Accession: phs000178). Molecular information of these tumours was obtained from the Pan-Cancer Atlas initiative (https://gdc.cancer.gov/about-data/publications/pancanatlas). Additional raw data is available from the senior author (P.A.V.D.V.) upon reasonable request. All custom scripts to perform the bioinformatic analyses are available via https://github.com/rjnell/um-rna.

Received: 23 September 2024; Accepted: 11 February 2025
Published online: 10 March 2025

References

1. Jager, M. J. et al. Uveal melanoma. *Nat. Rev. Dis. Prim.* **6**, 24. https://doi.org/10.1038/s41572-020-0158-0 (2020).
2. Furney, S. J. et al. SF3B1 mutations are associated with alternative splicing in uveal melanoma. *Cancer Discov.* **3**, 1122–1129. https://doi.org/10.1158/2159-8290.CD-13-0330 (2013).
3. Royer-Bertrand, B. et al. Comprehensive genetic landscape of uveal melanoma by whole-genome sequencing. *Am. J. Hum. Genet.* **99**, 1190–1198. https://doi.org/10.1016/j.ajhg.2016.09.008 (2016).
4. Van Raamsdonk, C. D. et al. Frequent somatic mutations of GNAQ in uveal melanoma and blue naevi. *Nature* **457**, 599–602. https://doi.org/10.1038/nature07586 (2009).
5. Van Raamsdonk, C. D. et al. Mutations in GNA11 in uveal melanoma. *N. Engl. J. Med.* **363**, 2191–2199. https://doi.org/10.1056/NEJMoa1000584 (2010).

6. Johansson, P. et al. Deep sequencing of uveal melanoma identifies a recurrent mutation in PLCB4. *Oncotarget* **7**, 4624–4631. https://doi.org/10.18632/oncotarget.6614 (2016).
7. Moore, A. R. et al. Recurrent activating mutations of G-protein-coupled receptor CYSLTR2 in uveal melanoma. *Nat. Genet.* **48**, 675–680. https://doi.org/10.1038/ng.3549 (2016).
8. Harbour, J. W. et al. Frequent mutation of BAP1 in metastasizing uveal melanomas. *Science* **330**, 1410–1413. https://doi.org/10.1126/science.1194472 (2010).
9. Harbour, J. W. et al. Recurrent mutations at codon 625 of the splicing factor SF3B1 in uveal melanoma. *Nat. Genet.* **45**, 133–135. https://doi.org/10.1038/ng.2523 (2013).
10. Martin, M. et al. Exome sequencing identifies recurrent somatic mutations in EIF1AX and SF3B1 in uveal melanoma with disomy 3. *Nat. Genet.* **45**, 933–936. https://doi.org/10.1038/ng.2674 (2013).
11. Prescher, G., Bornfeld, N., Horsthemke, B. & Becher, R. Chromosomal aberrations defining uveal melanoma of poor prognosis. *Lancet* **339**, 691–692 (1992).
12. Horsman, D. E. & White, V. A. Cytogenetic analysis of uveal melanoma. Consistent occurrence of monosomy 3 and trisomy 8q. *Cancer* **71**, 811–819 (1993).
13. Sisley, K. et al. Abnormalities of chromosomes 3 and 8 in posterior uveal melanoma correlate with prognosis. *Genes Chromosomes Cancer* **19**, 22–28. https://doi.org/10.1002/(sici)1098-2264(199705)19:1%3c22::aid-gcc4%3e3.0.co;2-2 (1997).
14. White, V. A., Chambers, J. D., Courtright, P. D., Chang, W. Y. & Horsman, D. E. Correlation of cytogenetic abnormalities with the outcome of patients with uveal melanoma. *Cancer* **83**, 354–359 (1998).
15. Damato, B. et al. Multiplex ligation-dependent probe amplification of uveal melanoma: correlation with metastatic death. *Invest. Ophthalmol. Vis. Sci.* **50**, 3048–3055. https://doi.org/10.1167/iovs.08-3165 (2009).
16. Smit, K. N. et al. Combined mutation and copy-number variation detection by targeted next-generation sequencing in uveal melanoma. *Mod. Pathol.* **31**, 763–771. https://doi.org/10.1038/modpathol.2017.187 (2018).
17. Thornton, S. et al. targeted next-generation sequencing of 117 routine clinical samples provides further insights into the molecular landscape of uveal melanoma. *Cancers (Basel)* **12**, 1039. https://doi.org/10.3390/cancers12041039 (2020).
18. Tschentscher, F. et al. Tumor classification based on gene expression profiling shows that uveal melanomas with and without monosomy 3 represent two distinct entities. *Cancer Res.* **63**, 2578–2584 (2003).
19. Zuidervaart, W. et al. Gene expression profiling identifies tumour markers potentially playing a role in uveal melanoma development. *Br. J. Cancer* **89**, 1914–1919. https://doi.org/10.1038/sj.bjc.6601374 (2003).
20. Onken, M. D., Worley, L. A., Ehlers, J. P. & Harbour, J. W. Gene expression profiling in uveal melanoma reveals two molecular classes and predicts metastatic death. *Cancer Res.* **64**, 7205–7209. https://doi.org/10.1158/0008-5472.CAN-04-1750 (2004).
21. Robertson, A. G. et al. Integrative analysis identifies four molecular and clinical subsets in uveal melanoma. *Cancer Cell* **32**, 204–220. https://doi.org/10.1016/j.ccell.2017.07.003 (2017).
22. de Lange, M. J. et al. Heterogeneity revealed by integrated genomic analysis uncovers a molecular switch in malignant uveal melanoma. *Oncotarget* **6**, 37824–37835. https://doi.org/10.18632/oncotarget.5637 (2015).
23. de Lange, M. J. et al. Digital PCR-based T-cell quantification-assisted deconvolution of the microenvironment reveals that activated macrophages drive tumor inflammation in uveal melanoma. *Mol. Cancer Res* **16**, 1902–1911. https://doi.org/10.1158/1541-7786.MCR-18-0114 (2018).
24. Alsafadi, S. et al. Cancer-associated SF3B1 mutations affect alternative splicing by promoting alternative branchpoint usage. *Nat. Commun.* **7**, 10615. https://doi.org/10.1038/ncomms10615 (2016).
25. Field, M. G. et al. Punctuated evolution of canonical genomic aberrations in uveal melanoma. *Nat. Commun.* **9**, 116. https://doi.org/10.1038/s41467-017-02428-w (2018).
26. Karlsson, J. et al. Molecular profiling of driver events in metastatic uveal melanoma. *Nat. Commun.* **11**, 1894. https://doi.org/10.1038/s41467-020-15606-0 (2020).
27. Nell, R. J. et al. Involvement of mutant and wild-type CYSLTR2 in the development and progression of uveal nevi and melanoma. *BMC Cancer* **21**, 164. https://doi.org/10.1186/s12885-021-07865-x (2021).
28. Nell, R. J. et al. Allele-specific digital PCR enhances precision and sensitivity in the detection and quantification of copy number alterations in heterogeneous DNA samples: an in silico and in vitro validation study. *medRxiv*, https://doi.org/10.1101/2023.10.31.23297362 (2023).
29. Nell, R. J. et al. Digital PCR-based deep quantitative profiling delineates heterogeneity and evolution of uveal melanoma. *medRxiv*. https://doi.org/10.1101/2024.01.30.24301871 (2024).
30. Cartegni, L., Chew, S. L. & Krainer, A. R. Listening to silence and understanding nonsense: Exonic mutations that affect splicing. *Nat. Rev. Genet.* **3**, 285–298. https://doi.org/10.1038/nrg775 (2002).
31. Mohn, F., Buhler, M. & Muhlemann, O. Nonsense-associated alternative splicing of T-cell receptor beta genes: No evidence for frame dependence. *RNA* **11**, 147–156. https://doi.org/10.1261/rna.7182905 (2005).
32. Repo, P. et al. Population-based analysis of BAP1 germline variations in patients with uveal melanoma. *Hum. Mol. Genet.* **28**, 2415–2426. https://doi.org/10.1093/hmg/ddz076 (2019).
33. Niersch, J. et al. A BAP1 synonymous mutation results in exon skipping, loss of function and worse patient prognosis. *iScience* **24**, 102173. https://doi.org/10.1016/j.isci.2021.102173 (2021).
34. Cole, Y. C. et al. Correlation between BAP1 localization, driver mutations, and patient survival in uveal melanoma. *Cancers (Basel)* **14**, 4105. https://doi.org/10.3390/cancers14174105 (2022).
35. Krug, A. K. et al. Improved EGFR mutation detection using combined exosomal RNA and circulating tumor DNA in NSCLC patient plasma. *Ann. Oncol.* **29**, 700–706. https://doi.org/10.1093/annonc/mdx765 (2018).
36. Schoofs, K. et al. Comprehensive RNA dataset of tissue and plasma from patients with esophageal cancer or precursor lesions. *Sci. Data* **9**, 86. https://doi.org/10.1038/s41597-022-01176-x (2022).
37. Albrecht, L. J. et al. Circulating cell-free messenger RNA enables non-invasive pan-tumour monitoring of melanoma therapy independent of the mutational genotype. *Clin. Transl. Med.* **12**, e1090. https://doi.org/10.1002/ctm2.1090 (2022).
38. Albitar, M. et al. Combining cell-free RNA with cell-free DNA in liquid biopsy for hematologic and solid tumors. *Heliyon* **9**, e16261. https://doi.org/10.1016/j.heliyon.2023.e16261 (2023).
39. van Poppelen, N. M. et al. SRSF2 mutations in uveal melanoma: a preference for in-frame deletions. *Cancers (Basel)* **11**, 1200. https://doi.org/10.3390/cancers11081200 (2019).
40. Rodrigues, M. et al. Outlier response to anti-PD1 in uveal melanoma reveals germline MBD4 mutations in hypermutated tumors. *Nat. Commun.* **9**, 1866. https://doi.org/10.1038/s41467-018-04322-5 (2018).
41. Johansson, P. A. et al. Prolonged stable disease in a uveal melanoma patient with germline MBD4 nonsense mutation treated with pembrolizumab and ipilimumab. *Immunogenetics* **71**, 433–436. https://doi.org/10.1007/s00251-019-01108-x (2019).
42. Katzir, R., Rudberg, N. & Yizhak, K. Estimating tumor mutational burden from RNA-sequencing without a matched-normal sample. *Nat. Commun.* **13**, 3092. https://doi.org/10.1038/s41467-022-30753-2 (2022).
43. Taylor, A. M. et al. Genomic and functional approaches to understanding cancer aneuploidy. *Cancer Cell* **33**, 676–689. https://doi.org/10.1016/j.ccell.2018.03.007 (2018).
44. Zoutman, W. H., Nell, R. J. & van der Velden, P. A. Usage of droplet digital PCR (ddPCR) assays for T cell quantification in cancer. *Methods Mol. Biol.* **1–14**, 2019. https://doi.org/10.1007/978-1-4939-8885-3_1 (1884).
45. Versluis, M. et al. Digital PCR validates 8q dosage as prognostic tool in uveal melanoma. *PLoS One* **10**, e0116371. https://doi.org/10.1371/journal.pone.0116371 (2015).

46. van Essen, T. H. et al. Prognostic parameters in uveal melanoma and their association with BAP1 expression. *Br. J. Ophthalmol.* **98**, 1738–1743. https://doi.org/10.1136/bjophthalmol-2014-305047 (2014).

Acknowledgements
This study is supported by the European Union's Horizon 2020 research and innovation program under grant agreement number 667787 (UM Cure 2020). We thank Ronald van Eijk (Department of Pathology, Leiden University Medical Center, Leiden, the Netherlands) for his help with the BAP1 DNA sequencing experiments. This work is partly based upon data generated by The Cancer Genome Atlas (TCGA) Research Network: https://www.cancer.gov/tcga.

Author contributions
R.J.N. and P.A.V.D.V. conceptualised and designed the study and wrote the manuscript. R.J.N. and M.V. performed the digital PCR experiments. R.J.N., D.C. and H.M. performed the bioinformatic analyses. R.M.V. and W.G.M.K. performed the additional diagnostic analyses regarding BAP1. G.P.M.L. and M.J.J. collected the patient materials. M.J.J. and P.A.V.D.V. acquired funding to perform the study. P.A.V.D.V. supervised the study. All authors reviewed the work and approved the final version of the manuscript.

Declarations

Competing interests
The authors declare no competing interests.

Additional information
Supplementary Information The online version contains supplementary material available at https://doi.org/10.1038/s41598-025-90122-z.

Correspondence and requests for materials should be addressed to R.J.N.

Reprints and permissions information is available at www.nature.com/reprints.

Publisher's note Springer Nature remains neutral with regard to jurisdictional claims in published maps and institutional affiliations.